Received: 8 July 2021 | Revised: 2 November 2021 | Accepted: 9 December 2021 | Published online: 28 January 2022

DOI: 10.1002/trc2.12241

Alzheimer's & Dementia
Translational Research & Clinical Interventions

RESEARCH ARTICLE

Diet-induced Alzheimer's-like syndrome in the rabbit

Craig Weiss[1] | Nicola Bertolino[2] | Daniele Procissi[2] | Grazia Aleppo[3] | Quinn C. Smith[1] | Kirsten L. Viola[4] | Samuel C. Bartley[4] | William L. Klein[4] | John F. Disterhoft[1]

[1] Department of Neuroscience, Northwestern University Feinberg School of Medicine, Chicago, Illinois, USA

[2] Department of Radiology, Northwestern University Feinberg School of Medicine, Chicago, Illinois, USA

[3] Division of Endocrinology, Metabolism and Molecular Medicine, Northwestern University, Feinberg School of Medicine, Chicago, Illinois, USA

[4] Department of Neurobiology, Northwestern University, Evanston, Illinois, USA

Correspondence
Craig Weiss, Department of Neuroscience, Northwestern University Feinberg School of Medicine, Ward Building 7-140, 303 E. Chicago Avenue, Chicago, Il 60611, USA.
E-mail: cweiss@northwestern.edu

Funding information
National Institutes of Health, Grant/Award Numbers: R56 AG050492, R01 NS113804, UL1TR001422, AG013854

Abstract

Introduction: Although mouse models of Alzheimer's disease (AD) have increased our understanding of the molecular basis of the disease, none of those models represent late-onset Alzheimer's Disease which accounts for >90% of AD cases, and no therapeutics developed in the mouse (with the possible exceptions of aduhelm/aducanumab and gantenerumab) have succeeded in preventing or reversing the disease. This technology has allowed much progress in understanding the molecular basis of AD. To further enhance our understanding, we used wild-type rabbit (with a nearly identical amino acid sequence for amyloid as in humans) to model LOAD by stressing risk factors including age, hypercholesterolemia, and elevated blood glucose levels (BGLs), upon an ε3-like isoform of apolipoprotein. We report a combined behavioral, imaging, and metabolic study using rabbit as a non-transgenic model to examine effects of AD-related risk factors on cognition, intrinsic functional connectivity, and magnetic resonance-based biomarkers of neuropathology.

Methods: Aging rabbits were fed a diet enriched with either 2% cholesterol or 10% fat/30% fructose. Monthly tests of novel object recognition (NOR) and object location memory (OLM) were administered to track cognitive impairment. Trace eyeblink conditioning (EBC) was administered as a final test of cognitive impairment. Magnetic resonance imaging (MRI) was used to obtain resting state connectivity and quantitative parametric data (R_2*).

Results: Experimental diets induced hypercholesterolemia or elevated BGL. Both experimental diets induced statistically significant impairment of OLM (but not NOR) and altered intrinsic functional connectivity. EBC was more impaired by fat/fructose diet than by cholesterol. Whole brain and regional R_2* MRI values were elevated in both experimental diet groups relative to rabbits on the control diet.

Discussion: We propose that mechanisms underlying LOAD can be assessed by stressing risk factors for inducing AD and that dietary manipulations can be used to assess etiological differences in the pathologies and effectiveness of potential therapeutics

against LOAD. In addition, non-invasive MRI in awake, non-anesthetized rabbits further increases the translational value of this non-transgenic model to study AD.

KEYWORDS
cholesterol, diabetes, eyeblink conditioning, late onset Alzheimer's disease, magnetic resonance imaging, whole-brain R_2*

1 | INTRODUCTION

Although mouse models of Alzheimer's disease (AD) have increased our understanding of the molecular basis of the disease, none of those models represent late-onset Alzheimer's Disease which accounts for >90% of AD cases[1,2], and no therapeutics developed in the mouse (with the possible exceptions of aduhelm/aducanumab[3] and gantenerumab[4,5]) have succeeded in preventing or reversing the disease.[6,7] Late-onset AD (LOAD) is particularly challenging to study using mouse models because it is not linked to any known genetic mutations, but it is affected by several risk factors including age, hypercholesterolemia, Type 2 diabetes, and the ε4 allele of apolipoprotein E (*APOE*). Challenges associated with development of effective treatments are linked to the complex multi-factorial, multi-pathway etiology driving its pathophysiological progression. Identifying mechanisms and links among these risk factors can provide new avenues for therapeutic development.

Given that the amino acid sequence for amyloid is nearly identical between rabbits and humans,[8] the physiology of lipids is more similar between rabbits and humans than between mice and humans,[9] and that working with non-human primates such as marmoset can be difficult, we selected wild-type (WT) rabbit as a non-transgenic mammalian model to avoid off-target effects of inserting foreign DNA into the genome,[10] and to evaluate the effects of AD-related diet-based risk factors (high cholesterol or an elevated blood glucose level) on cognition and intrinsic functional connectivity within neural networks of the rabbit brain as detected by resting state functional magnetic resonance imaging (fMRI). The rabbit AD model offers several advantages. Among these is the five decade–long use of the rabbit to study learning and memory of eyeblink conditioning (EBC).[11–14] Importantly, EBC is impaired by AD, even in relation to normal age-related impairment.[15] Rabbits exhibit AD-like pathology in response to a diet enriched with cholesterol and copper,[16] further strengthening the argument in favor of its potential to be used to study LOAD. We replicated the cholesterol and copper diet in aging rabbits, added a group fed a diet enriched with saturated fat and fructose, and expanded characterization of memory by adding recognition tests that can be done repeatedly simply by using different objects or locations with each repeat of the test.[17]

Having shown[18] that resting state fMRI (rsfMRI) in awake rabbits provides reliable information on brain intrinsic functional connectivity networks, we acquired and compared connectivity data across groups to determine diet-related differences among functional networks. Finally, using MRI to generate R_2* ($1/T_2$*) brain maps we measured whole-brain and regional R_2* values that were consistently higher in the diet groups compared to the control group. These changes (i.e., increases in R_2* and decreases in T_2*) are interpreted as possible increases in iron depositions that co-localize with amyloid within the brain of rabbits undergoing these diets.[19,20] We propose that diet-induced cognitive impairment and awake fMRI in the WT rabbit are powerful tools for testing potential therapeutics and for validation of diagnostic imaging biomarkers in a translationally relevant AD perspective.

2 | METHODS

2.1 | Animals

Given that age is the major risk factor for acquiring sporadic AD, and that rabbits exhibit significant age-related impairments in acquiring hippocampal-dependent trace EBC as early as 24 months of age,[21,22] we selected aging New Zealand White rabbits for this experiment (30 ± 2.6 months at start of experiment). Only female rabbits were available from the vendor (Covance) as retired breeders. Two consecutive cohorts of 12 rabbits were used, and all three diets were represented in both cohorts. However, two rabbits on cholesterol did not complete the schedule due to liver and vascular complications and one rabbit assigned to the fat/fructose diet was a statistical outlier in terms of its performance during trace EBC; those rabbits were excluded from the analyses. The final tally of rabbits per group was six on cholesterol diet, seven on fat/fructose diet, and eight on normal control diet.

2.2 | Diets

Rabbits were assigned to one of three Tekland diets: normal rabbit chow (#8630), normal chow with 2% cholesterol and 2% molasses for flavoring (#621107), or normal chow with 10% saturated fat (coconut oil) and 30% fructose (#621103). Rabbits had ad lib access to reverse osmosis water; the water of rabbits in the cholesterol group was spiked with 0.12 ppm copper.[16]

Rabbits in each group were offered 300 kcal/d of food to dissociate calories from the effects of the specific diet (rabbits on cholesterol often failed to consume all their daily feed; molasses flavoring partially rescued the inappetence).

2.3 | Blood chemistry

Blood was taken from the marginal ear vein monthly to acquire a metabolic profile. Serum was separated from clotted blood by

centrifugation, stored on ice, and shipped to an independent laboratory for a lipid profile assay. A glucose tolerance test was performed after 21 or 24 weeks on diet (cohorts 1 and 2, respectively) and blood was sampled throughout a period of 2 hours.

2.4 | Novel recognition tests

Cognition was assessed monthly using novel object recognition (NOR) and object location memory (OLM) to track progression of memory impairment.[17] A memory index score was calculated for each test using the formula: (investigation time of novel cue or position–investigation time of familiar cue or position)/(investigation time of novel cue or position + investigation time of familiar cue or position). Results from the first set of tests were used to assign each rabbit to a diet group so that baseline memory index scores were similar among the three groups before beginning the experimental diets.

2.5 | Eyeblink conditioning

Rabbits were surgically prepared[23,24] and tested for EBC after they completed ≈ 5 months of diet and repeated memory assays with NOR and OLM. The conditioning stimulus (CS) was a vibration (250 milliseconds, 62.5Hz) of the B row of whiskers on the right side of the face. The unconditioned stimulus (US) was a 150 millisecond puff of nitrogen (150 milliseconds, 3 to 5 psi) presented to the cornea of the right eye. A stimulus-free interval of 500 milliseconds was inserted between the end of the CS and onset of the US. Movement of the nictitating membrane (NM, third eyelid) was detected with a reflective infrared sensor after holding the eyelids open with tailor hooks. Extensions of the NM after CS onset and before US onset were considered conditioned responses (CRs) if the signal change was at least 4 standard deviation (SD) greater than the mean of the 250 millisecond baseline signal for at least 15 milliseconds. Each daily session of EBC presented 80 trials with a random intertrial interval ranging between 30 and 60 seconds.

2.6 | MRI acquisition

Images were acquired with a 7T ClinScan MRI scanner, as recently reported.[18] A three-channel custom-made receiver coil (RAPID MR International) designed with a central aperture was used. The volume quadrature coil was used for transmission. The acquisition protocol included a coronal 3D-GRE multi-echo scan with repetition time (TR) = 68 milliseconds and echo times (TEs) as used previously.[18]

2.7 | MRI data analysis

Images were analyzed using FMRIB Software Library version 6.0 (Analysis Group, FMRIB), FSLNets 0.6, and MatLab R2017a (The Mathworks Inc.), as we did previously.[18]

RESEARCH IN CONTEXT

1. Systematic Review: The authors reviewed relevant literature using PubMed sources and meeting abstracts and presentations.
2. Interpretation: Our results demonstrate that dietary risk factors for Alzheimer's disease (AD) in a non-transgenic animal can be used to induce AD-like memory impairment, altered intrinsic functional connectivity, and whole-brain and regional increases in quantitative R_2*.
3. Future Directions: Future work will address histopathological changes related to the cognitive impairment and magnetic resonance imaging-derived results, that is, altered functional connectivity and regional R_2* increases to identify cellular and sub-cellular changes more specifically. The described model will also be used to analyze quantified histopathological changes based on the ATN criteria of amyloid, tau, and neurodegeneration,[2] and to test potential therapeutics against cognitive impairments and neuropathology.

For the resting state analysis, echo planar images (EPIs) were preprocessed: (1) all volumes were registered by a rigid transformation to the central volume and motion regressors were removed from the data to limit motion artifacts effect, (2) a brain mask was generated starting from the bias field corrected mean of the volumes and used as an inclusive mask for EPI, (3) a common origin was selected for all subjects' EPIs, (4) time course data were high-pass filtered with a threshold of 0.02 Hz, and (5) images were smoothed using a 0.7 millimeter Gaussian kernel. The better of the two MRI acquisitions from each rabbit (based on visual inspection of EPI volumes and motion correction reports) was chosen for further analysis. Functional volumes were registered to high-resolution 3D images and then to the common template before independent components analysis (ICA). ICA was run using a multi-session temporal concatenation pre-selecting 30 desired components. Resulting components were inspected to identify resting state and spurious components.

Statistical differences among diet groups were explored using dual-regression analysis (corrected for multiple comparison using 5000 permutations). A network analysis was performed on time courses extracted from stage 1 output to assess correlations among the resting state components across all subjects. For each rabbit a matrix of Pearson correlation coefficients was calculated, transformed using the Fisher *z*-transform and a cross-subject general linear model (GLM) analysis was performed to explore differences among groups. We also computed the average correlation matrix for each diet group, applied a threshold of $r > 0.2$, created diet group network graphs, and computed the network efficiencies.

Parametric R_2* maps were generated for each rabbit using a voxel-by-voxel, least-square fitting tool included in the image processing

software Jim (Xinapse). R_2^* was used for analysis instead of $1/T_2^*$ because the former is directly proportional to iron deposition and R_2^* values are associated with cognitive impairment even during normal brain aging[19] while T_2^* maps are linked to iron oxide deposition in a more complex way. Co-registration of all images was accomplished using the built-in elastic co-registration tools. To conduct robust quantitative comparison of R_2^* data from each experimental group we used a R_2^* digital quantitative reference map generated previously using data from multiple healthy control rabbits (n = 24, from previous experiments) as an absolute baseline. Using whole brain and regional R_2^* values from this baseline parametric map we computed averaged normalized R_2^* quantities using the formula $\frac{\Delta R_2^*}{R_2^*} = \frac{(R_2^* - R_{2-baseline}^*)}{R_{2-baseline}^*}$. We determined intrinsic variability of our measurements (by comparing baseline to control group) to detect possible regional R_2^* diet-induced changes in the fat/fructose and cholesterol diet groups.

The average R_2^* whole brain was calculated excluding ventricles to eliminate bias in the quantitative assessment. The average regional R_2^* values were extracted from the MRI parametric brain maps after realignment and co-registration of all maps.

2.8 | Immunofluorescence labeling of tissue slices

Rabbits were perfused (4% paraformaldehyde in phosphate-buffered saline, pH 7.4) and the brain was post-fixed 1 week, followed by 10% sucrose for 3 days, then 20% sucrose for at least 3 days (0.02% sodium azide was added to solutions). Brains were stored in 20% sucrose solution until sliced (45 μm) for immunohistochemistry. Details of immunostaining are in the figure legends.

3 | RESULTS

3.1 | Effects of diets on blood chemistries

Figure 1 shows blood chemistry results across time. Results confirm success of the diet-induced model for hypercholesterolemia and for elevated levels of blood glucose as present with Type 2 diabetes. Rabbits on the cholesterol enriched diet had a large, statistically significant, and persistent increase in serum cholesterol as early as 1 month on diet (Figure 1A, $F_{2,19} = 245.3$, $P < .0001$). The average cholesterol level across time was >1000 mg/dL; rabbits on control diet averaged 29.5 mg/dL; rabbits on the fat/fructose diet averaged 49.5 mg/dL. The overall difference between the fat/fructose diet and control diet was not statistically significant. The two rabbits from the cholesterol group that did not complete the study had serum cholesterol levels > 1500 mg/dL and signs of liver toxicity. This result led us to invoke cholesterol-free days for all rabbits assigned to that diet starting at week 16 on diet. Normal chow was given during weeks 16 to 18, and again during weeks 20 and 24. This feeding schedule maintained an elevated level of serum cholesterol and prevented liver toxicity.

Rabbits on the fat/fructose diet exhibited a statistically significant and persistent elevation in blood glucose levels (BGLs) as of 1 month on diet (Figure 1B). The level exceeded 126 mg/dL, that is, the value that is diagnostic of diabetes in humans. Rabbits on cholesterol also attained a BGL >126, that is, 128 mg/dL, but not until after 4 months on diet; rabbits on control diet did not exceed 126 mg/dL BGL. Differences in BGL among the groups were statistically significant according to repeated measures analysis of variance (ANOVA; $F_{2,19} = 8.6$, $P = .0022$) and were detected as early as 1 month from start of the diet (fat/fructose: 133.7 ± 4.2, cholesterol: 115.9 ± 2.4, control: 113.8 ± 2.4). Post hoc Fisher's tests indicated that the BGL of rabbits on the fat/fructose diet was significantly greater than the BGL from rabbits on either the control or cholesterol diets ($P = .0042$ and $P = .013$, respectively). The fat/fructose diet was also associated with an increase in circulating triglycerides ($F_{2,19} = 7.7$, $P = .0035$) due to an increase in the rabbits on the fat/fructose diet (Figure 1C). A persistent and significantly elevated triglyceride level was seen after 1 month on diet and is predictive of amyloid and tau pathology years later in humans.[26] Rabbits on control diet had a mean triglyceride level of 48.4 ± 3.2 mg/dL that did not change significantly across time. Rabbits on fat/fructose diet had a mean level of 170.7 ± 19.3 from 1 to 4 months on the diet. The mean triglyceride level of rabbits on the cholesterol diet spiked on

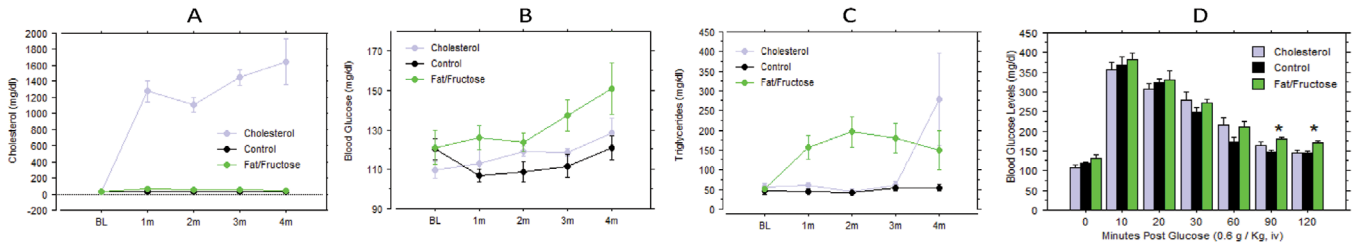

FIGURE 1 Experimental diets induced either hypercholesterolemia or elevated blood glucose levels, as intended. A, Monthly lipid profiles revealed hypercholesterolemia induced by the diet enriched with 2% cholesterol (and 0.12 ppm copper in their purified [RO] drinking water). B, Elevated blood glucose levels (as associated with Type 2 diabetes) was achieved in rabbits on a diet enriched with 30% fructose and 10% saturated fat (as coconut oil), that is, blood glucose level (BGL) >126 mg/dL. C, Diet significantly affected triglyceride levels due to an increase in the rabbits on the fat/fructose diet. D, A glucose tolerance test was done at either 21 or 24 weeks after the start of the diets (cohorts 1 and 2, respectively). Post hoc analysis of variance for each timepoint after the glucose injection revealed that rabbits on the fat/fructose diet exhibited impaired glucose tolerance relative to the other groups at 90 and 120 minutes after the glucose injection

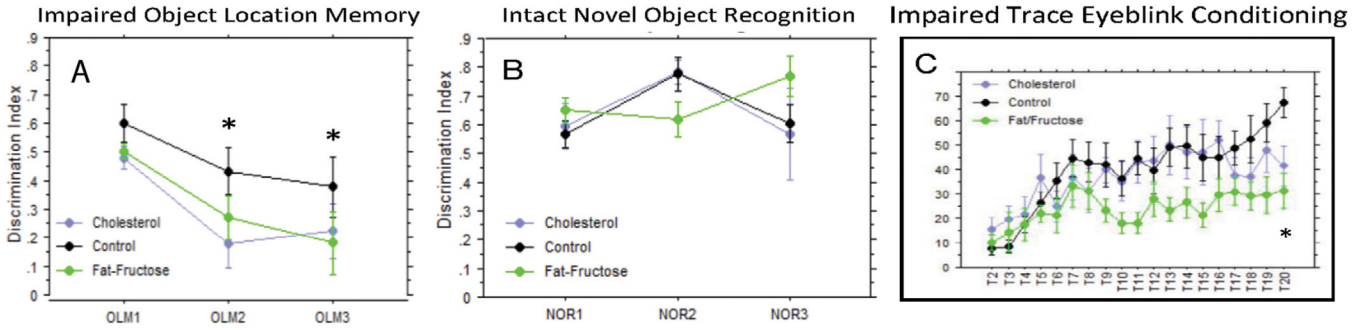

FIGURE 2 Differential effects of experimental diets on cognitive behaviors. Shown are plots of discrimination scores for object location (A) and for object recognition (B) across time (baseline, week 5, week 11). A score of 1.0 indicates investigation of only the novel location or novel object; a score of 0.0 indicates equal investigation times for both locations or objects. An analysis of variance (ANOVA) revealed a statistically significant difference for object location memory among the diet groups. C, Trace eyeblink conditioning (EBC) was significantly impaired by both experimental diets, but much more so by the fat/fructose diet. Post hoc least significant difference (LSD) tests revealed that rabbits on the fat/fructose diet exhibited significantly fewer conditioned responses (CRs) than rabbits on either the control or cholesterol-enriched diet ($P = .037$). An ANOVA on the percent of CRs during the final session of trace EBC confirmed a significant difference among the groups ($F_{2,18} = 7.6$, $P = .004$) and post hoc LSD tests revealed that rabbits on either the cholesterol or fat/fructose diet exhibited significantly fewer CRs than rabbits on the control diet ($P = .019$, $P = .001$, respectively)

the last reading due to a large increase in two rabbits at that timepoint, that is, 711 and 576 mg/dL.

The fat/fructose diet also impaired glucose tolerance (Figure 1D) as revealed by repeated samplings of BGL after the injection of 0.6 g/Kg glucose (iv). An ANOVA of pretest baseline values revealed a non-statistically significant elevation in BGL due to the fat/fructose diet (130.3 vs. 118.9 [controls] and 108.3 [cholesterol], $F_{2,19} = 2.2$, $P = .137$), and post hoc ANOVA for each time point after the glucose injection revealed that rabbits on the fat/fructose diet exhibited impaired glucose tolerance relative to the other groups at 90 and 120 minutes after the glucose injection ($F_{2,19} = 6.6$, $P = .0065$ and $P = .0064$ for the 90 and 120 minutes timepoint, respectively, comparison by Fisher's predicted least significant difference test).

3.2 | Experimental diets impair hippocampal-dependent memory

3.2.1 | Spatial and object memory

High-fidelity spatial memory requires the hippocampus (and not perirhinal cortex) while object recognition requires the perirhinal cortex (and not hippocampus).[27–30] Both experimental diets significantly impaired spatial memory, as determined with the assay for OLM ($F_{2,21} = 3.9$, $P = .036$). Rabbits on both the cholesterol-enriched diet and the fat/fructose–enriched diet had significantly poorer memory for object location based on discrimination index scores according to post hoc least significant difference test ($P = .0173$ and .0372, respectively, Figure 2A). The impairment was present after 5 weeks of diet and persisted through 11 weeks of diet (Figure 2A). Novel object recognition was not significantly impaired by either diet (Figure 2B).

3.2.2 | Temporal associative memory

Both experimental diets impaired forebrain- and cerebellar-dependent trace EBC.[28–35] Acquisition is also impaired by aging in rabbits[21,22] and humans.[36,37] Rabbits on the fat/fructose diet acquired trace EBC at a significantly slower rate than the rabbits on either the control diet or the cholesterol-enriched diet (Figure 2C), and both diet groups performed significantly worse than rabbits on the control diet during the final conditioning session. A two-way repeated-measures ANOVA for the percent of CRs revealed a significant interaction of diet group and days of conditioning ($F_{36,324} = 1.68$, $P = .011$). Post hoc least significant difference (LSD) tests revealed that rabbits on the fat/fructose diet exhibited significantly fewer CRs than rabbits on either the control or cholesterol-enriched diet ($P = .037$). An ANOVA on the percent of CRs during the final session of trace EBC confirmed a significant difference among the groups ($F_{2,18} = 7.6$, $P = .004$) and post hoc LSD tests revealed that rabbits on either the cholesterol or fat/fructose diet exhibited significantly fewer CRs than rabbits on the control diet ($P = .019$, $P = .001$, respectively).

3.3 | Experimental diets reduce intrinsic connectivity among resting-state brain networks

An analysis of the intrinsic functional connectivity data among neural networks in the rabbit brain at rest[24] replicated previous results,[35] except for independent bilateral cerebellar networks instead of one common cerebellar network. The 10 independent networks are shown in Figure 3A. The correlation matrix for all the nodes for each diet group is shown in Figure 3B, and a ball-and-stick connectivity map of the network for each diet is shown in Figure 3C. Note that the retrosplenial cortex is a major node in the network, that the fat/fructose diet greatly

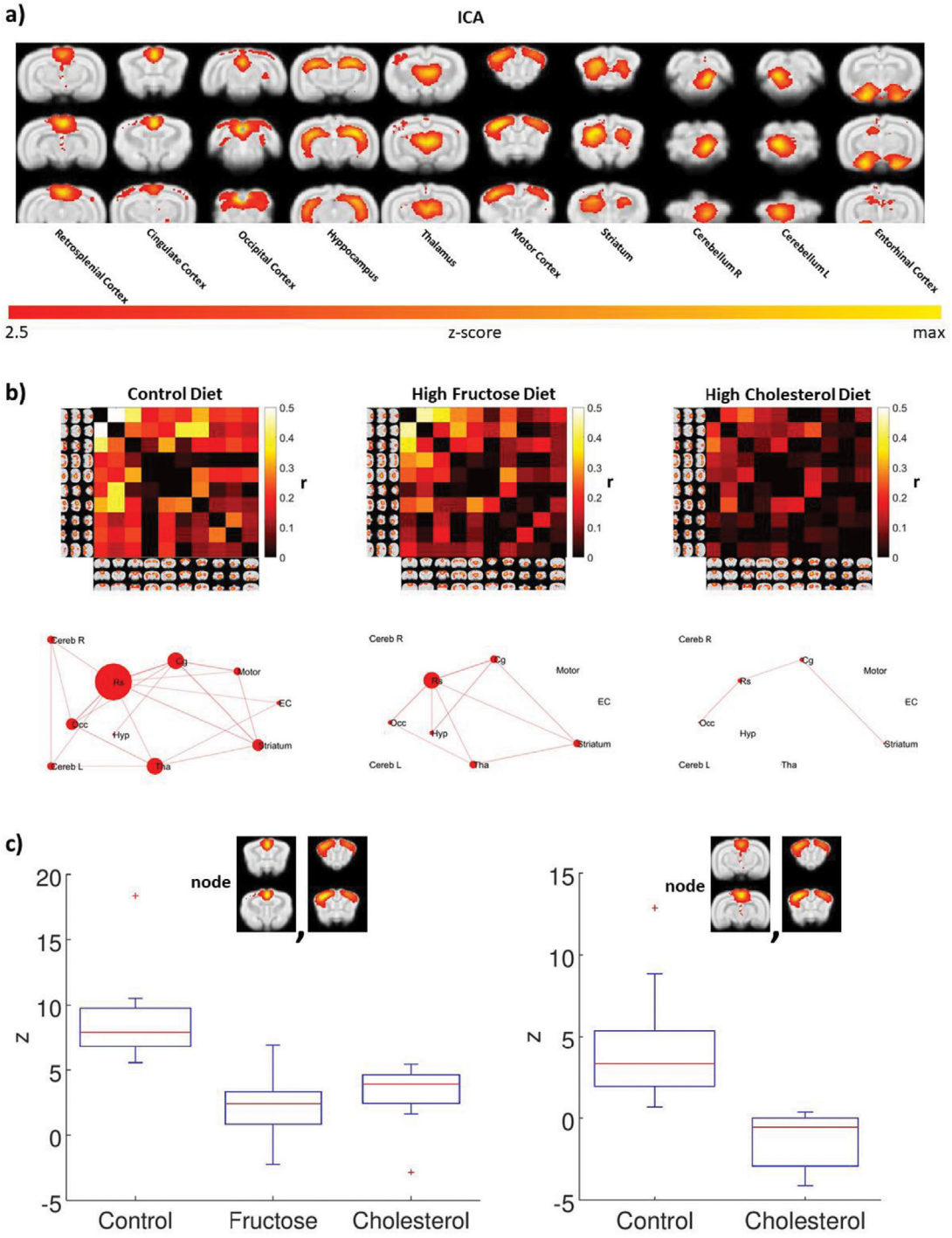

FIGURE 3 Experimental diets alter intrinsic brain connectivity in awake rabbit, as assayed with functional magnetic resonance imaging. A, Group independent components analysis analysis of all animals identified 10 resting state components: retrosplenial cortex, cingulate cortex, occipital cortex, hippocampus, thalamus, motor cortex, striatum, right cerebellum, left cerebellum, and entorhinal cortex. B, Differences and interactions among the network nodes can be assessed visually with the color intensity matrices and ball-and-stick graphs. C, A general linear model analysis of the correlation matrices revealed significant differences in three contrasts: control group > fructose group in the correlation between the cingulate cortex and the motor cortex ($P_{corrected} < .05$); control group > cholesterol group in the correlation between cingulate cortex and motor, and in the correlation between retrosplenial cortex and motor cortex ($P_{corrected} < .05$). The fructose group is not represented because there was no significant functional connectivity between retrosplenial cortex and motor cortex for this diet group. Red crosses represent values >1 standard deviation from the mean

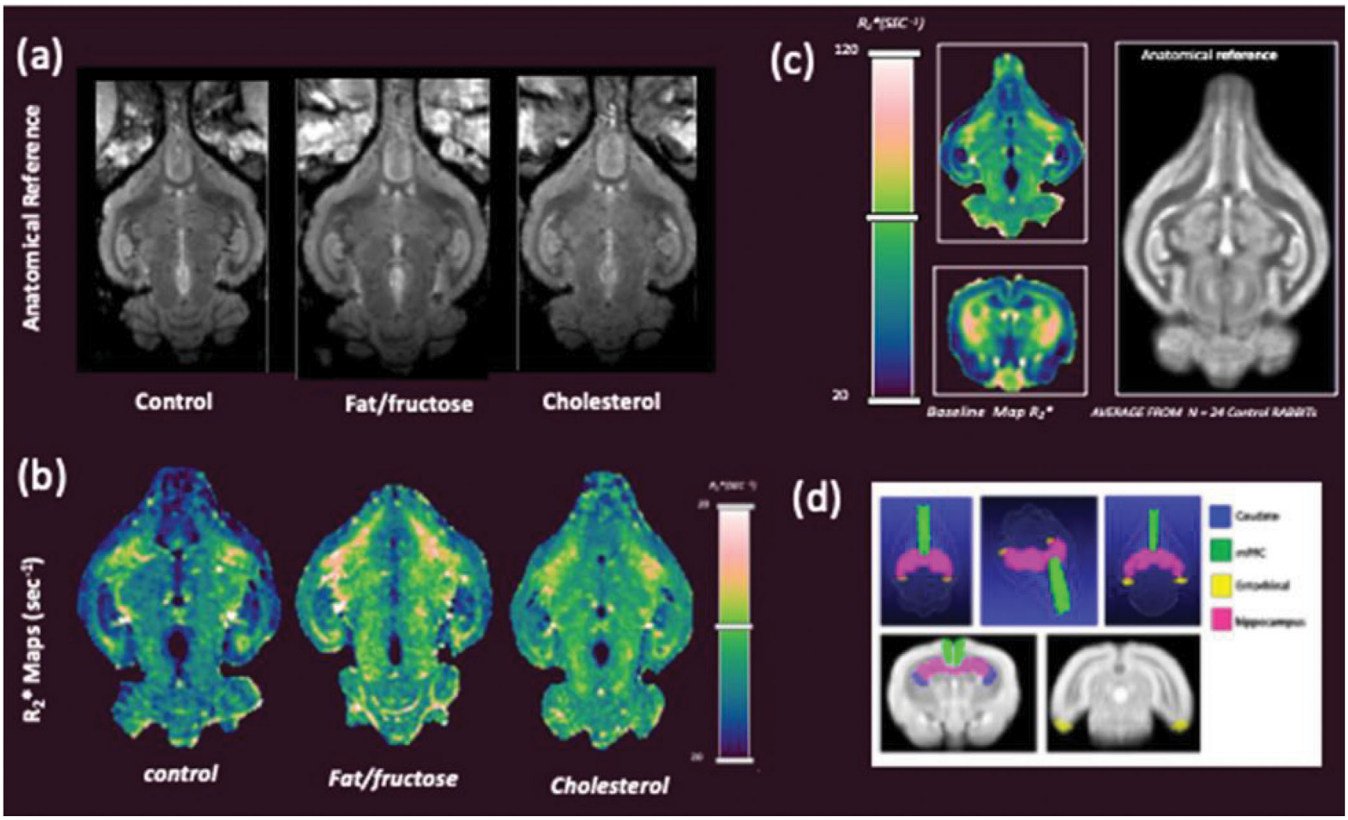

FIGURE 4 Representative anatomical (A) and R_2*images (B) for each group of rabbits. C, Baseline R_2* map example (longitudinal and coronal) used for comparative analysis and corresponding anatomical image; image at right shows our digital reference standard compiled from 24 control rabbits. D, 3D rendering and 2D images showing regions of interest used to extract quantitative values for analysis

reduces connectivity between it and the rest of the network, and that the fat/fructose diet functionally disconnects the cerebellum, entorhinal cortex, and motor cortex from each other and the rest of the network. Efficiencies of the network among resting state components[39] were: 0.7 (controls), 0.27 (fat/ fructose), and 0.1 (cholesterol).

Effects of cholesterol on network connectivity were remarkable. It greatly reduced connectivity among nodes and effectively isolated the entorhinal cortex, hippocampus, retrosplenial cortex, and cerebellum from each other (Figure 3B). Analyses using a GLM model indicated that relative to the control diet, both experimental diets significantly reduced connectivity in the cingulo-motor network (Figure 3C); cholesterol also significantly reduced connectivity in the retrosplenial-motor network. The GLM correlation matrices revealed significant differences in three contrasts: fructose < control in the correlation between the cingulate cortex and the motor cortex ($P_{corrected} < .05$), cholesterol < control in the correlation between cingulate cortex and motor, and in the correlation between retrosplenial cortex and motor cortex ($P_{corrected} < .05$).

Shown in Figure 4A are MR images showing representative longitudinal anatomical views from each group. The corresponding R_2* maps are shown in Figure 4B. Shown in Figure 4C is a representative coronal and axial R_2* parametric image from our baseline data set (n = 24 control rabbits). Regions with higher R_2* values (or lower T_2* values) compared to control group (and baseline) are notable in Figure 4B in both diet-fed cohorts. Figure 4D depicts qualitative 2D and 3D renderings showing the regions of interest used for quantitative analysis.

3.4 | Experimental diets yield immunohistochemical markers of AD-like neuropathology

An in-depth histopathological evaluation is beyond the scope of this study. However, we show examples for both amyloid oligomers and phospo-tau for each diet group in Figure 5. The CA fields and the dentate gyrus of hippocampus were stained with ACU193 or NU2 (for amyloid oligomers) and with AT8 for phosphorylated tau (p-tau). These examples suggest that amyloid oligomers and p-tau become elevated in the hippocampus of aging rabbits fed with special diets compared to the control diet, in agreement with our reported behavioral, rsfMRI connectivity, and R_2* quantitative analyses.

4 | DISCUSSION

The results support the use of rabbits as an animal model to study the involvement of risk factors related to the genesis of AD-like cognitive deficits and alterations of intrinsic connectivity. The human-like

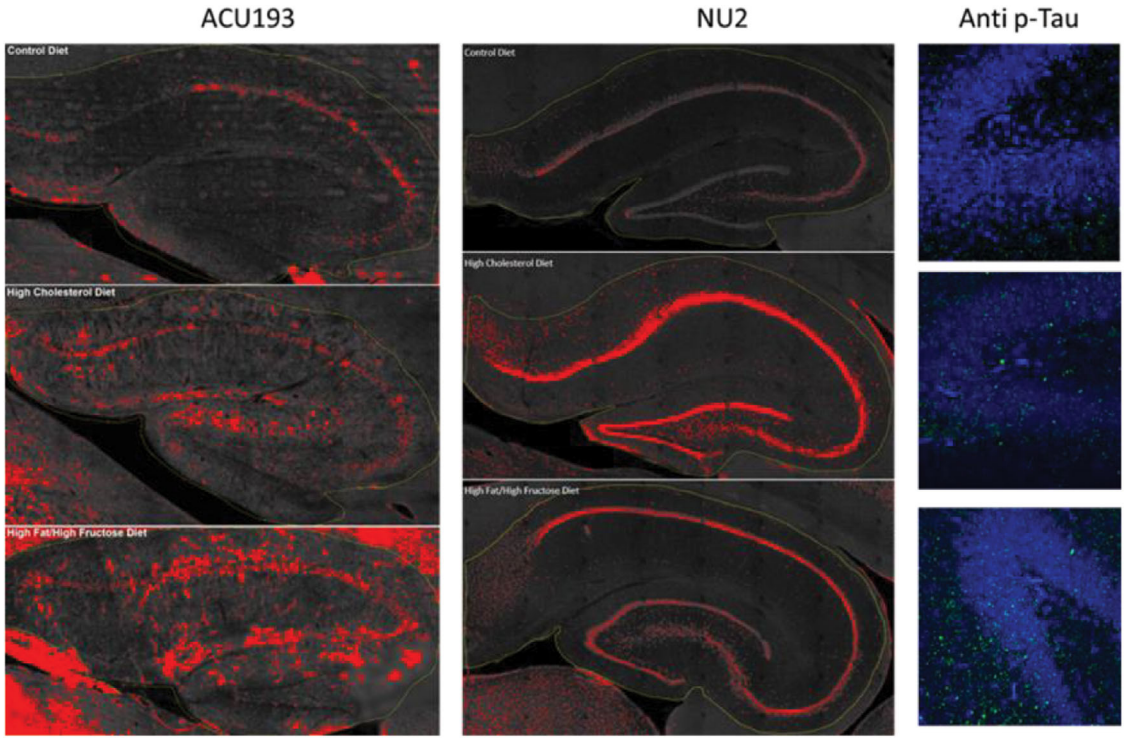

FIGURE 5 Experimental diets increase Alzheimer's disease–related pathology detected using immunohistochemical fluorescence detection. Examples of immunohistochemical staining for amyloid oligomers (ACU193 and NU2) and phosphorylated tau (AT8 p-tau) in hippocampus of rabbits that were fed the control diet (top row), a diet enriched with 2% cholesterol (middle row), or a diet enriched with 10% saturated fat and 30% fructose (bottom row). ACU193 and NU2 (left and center, respectively) were imaged using the Lionheart automated microscope. Images collected from a full-slide scan at 10× were stitched together, then regions of interest were thresholded uniformly using ImageJ. Red on the images denotes specific signal above the determined threshold for the set of images. AT8 (right) images were collected using the Leica SP8 confocal microscope at 63×. Data shows an increase in AT8 (green) positive sites in the dentate gyrus of experimental diet animals over signal detected in the control diet animals. Increased p-tau was also seen in other hippocampal regions as well as frontal and temporal cortex (data not shown). Selected slices were washed with Tris-buffered saline (TBS) three times for 10 minutes each, permeabilized with 0.3% Triton X-100 (Sigma) in TBS (working buffer) for 30 minutes at room temperature, then blocked with 10% normal goat serum (NGS) diluted in working buffer for 60 minutes at room temperature. Slices were incubated with ACU193, a humanized monoclonal antibody against AβOs, at 1 μg/mL, or NU2, a mouse monoclonal against AβOs,[25] at 1.5 μg/mL, or AT8, anti-phospho tau (Ser 202, Thr 205) (Invitrogen), at 1:500 diluted in 10% NGS. Slices were incubated at 4°C for 3 days on an orbital shaker. After washing three times for 30 minutes each with working buffer at room temperature, slices were incubated with the AlexaFluor secondary (Invitrogen), anti-human for ACU193 or anti-mouse for AT8 and NU2, diluted 1:2000 in 1% NGS working buffer at 4°C overnight. Slices were washed three times (15 minutes each) in TBS, then mounted on SuperFrost slides. Images were collected using the Leica TCS SP8 confocal microscope or BioTek Lionheart FX microscope

amino acid sequence for rabbit amyloid; structural similarity of rabbit and human tau; human-like lipid physiology; an *APOE* sequence that is 80% homologous to the *APOE* ε3 isoform,[40] the most common isoform in humans; and a spontaneous ability for rabbits to develop Type 2 diabetes,[41] make the rabbit a good model to study the genesis of AD and the effects of potential therapeutics. The rabbit provides an additional tool alongside murine genetic models to investigate more thoroughly the underlying mechanisms and causes of AD.

In our study, WT rabbits allowed an examination of diabetic-like changes without the use of the relatively rare heritable hyperlipidemia exhibited in the Watanabe rabbit,[42] which has a deletion of the binding domain of the low-density lipoprotein receptor[43] and which has been used to examine mechanisms related to high cholesterol[44] and Type 2 diabetes.[42] Each diet produced the expected results in blood chemistries, and similar impairments on OLM, but differential effects on forebrain-dependent trace EBC were found, that is, rabbits on fat/fructose were impaired, while rabbits on the high cholesterol diet were not impaired until late in training; and differential effects on functional connectivity were found, that is, cholesterol dramatically dissociated functional connectivity among the nodes of the retrosplenial-motor network while the fat/fructose diet impaired functional connectivity within the cingulo-motor network, but to a lesser degree than the effect of cholesterol on the retrosplenial-motor cortex network.

As reported by the Ronald laboratory,[45] cholesterol-enriched diet in rabbits was associated with signal voids and hypointensities in T_2*-weighted MRI. Correlation of the MRI hypointense regions with iron-rich regions (according to Prussian blue staining) suggests a link with amyloid plaque formation as reported by immunohistochemistry data.[45] While interpretation of these quantitative changes has not achieved widespread consensus, the presence of hypointense regions

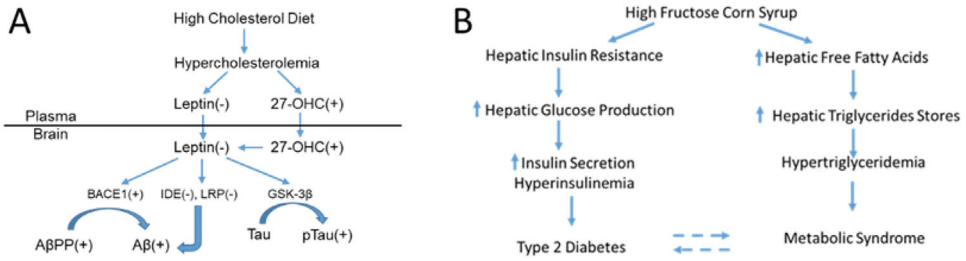

FIGURE 6 Metabolic pathways mediating pathological effects of (A) cholesterol- or (B) fructose-enriched diets that lead to increased amyloid, phosphorylated tau, Type 2 diabetes, and metabolic syndrome. Panel A was adapted from Marwarha et al.[48]

in T_2*-weighted MR images is linked to cellular-level changes and could potentially reflect onset of amyloid neurodegenerative progression. For this reason, we quantitatively analyzed parametric R_2* maps, that is, 1/T_2*, extracting both whole-brain as well as regional averages for each cohort of rabbits with the goal of detecting R_2* patterns that could reflect the neurodegenerative progression in our diet-based models. Interestingly, the results showed relative trends across groups that were similar to those observed in the behavioral data, with overall increase of R_2* in both diet groups compared to the control group throughout the brain. Overall, these results suggest that understanding etiological differences among people diagnosed with AD might lead to more specific treatments for each etiology.

A convergence of different etiologies onto common pathological mechanisms might occur at the level of glycogen storage and/or mitochondrial function in which metabolism and energy production intersect in neurons and glia. Increased absorption of glucose leads to increased release of insulin and increased availability of glucose to cells. However, high-fructose corn syrup in the modern diet drives metabolism toward glycogen storage and an increased likelihood for metabolic syndrome and diabetes, especially when combined with a high-fat diet as we have used here. High-fat diet in rats has been shown to impair a hippocampal-dependent object location task[46] and spontaneous alternation and intrinsic excitability of hippocampal CA1 pyramidal neurons[47] which is required for neuroplasticity and acquisition of trace EBC. Those changes could be related to the impaired EBC and resting state functional connectivity reported here, and which may serve as biomarkers for potential therapeutics for the treatment of cognitive impairments.

At the molecular level, increased serum cholesterol decreases the concentration of leptin, which then drives an increase in beta amyloid cleaving enzyme (BACE1) and a decrease in insulin-degrading enzyme, both of which increase the production of amyloid beta. Interactions with leptin have been studied in the rabbit and in organotypic slices of rabbit hippocampus.[45] Decreasing levels of leptin also drive the phosphorylation of tau (Figure 6). The fat/fructose diet also promotes the development of Type 2 diabetes and metabolic syndrome, fructose in particular, and its increased use via high-fructose corn syrup is associated with increased neurodegeneration and tau deposition.[49]

Combining the rabbit model with additional transgenic models has the potential to provide a comprehensive set of tools for multi-scale characterization of molecular mechanisms underlying AD pathophysiology and the effects of potential therapeutics on progression of the disease. In addition, our model can be used effectively for comprehensive therapeutic testing of novel treatments through the use of behavioral tests (i.e., the temporal association trace EBC assay and the object location test), and through MRI detection of iron oxide labeled agents that target amyloid oligomers (an early biomarker for AD) as reported for rabbits injected with synthetic amyloid oligomers.[50]

ACKNOWLEDGMENTS

We thank Nicholas Rozema and Mary Kando for help with rabbit behavioral studies. Microscopy was performed at the Biological Imaging Facility at Northwestern University (RRID:SCR_017767), graciously supported by the Chemistry for Life Processes Institute, the NU Office for Research, and the Department of Molecular Biosciences and the Rice Foundation. Funded in part by: National Institutes of Health R56 AG050492, R01 NS113804, UL1TR001422, AG013854. Eleanor Wood Prince Grant from the Woman's Board of Northwestern Memorial Hospital.

CONFLICTS OF INTEREST

Grazia Aleppo is partially supported by Novo-Nordisk, Eli-Lilly, and Insulet/Dexcom. Payments to William L. Klein were made to organize a meeting for Acumen Pharmaceuticals. William L. Klein has founders' shares in Acumen Pharmaceuticals and is a member of the scientific advisory board of Acumen. ACU193 was a gift from Acumen Pharmaceuticals. NU2 was developed with support from NIH Grants RO1AG18877 and RO1AG22547 to Northwestern University. Support paid to Northwestern University from NIH R01 AG063903, NIH-R21 AG060203-01, NIH-R43OD023025-01A1 (subcontract from Virscio, Inc). Imaging partially supported by the Rice Foundation. John F. Disterhoft supported by NIH R01 NS113804, R01 MH114923, R25 GM121231, T32 AG20506-16-20, RF1 AG017139, R37 AG008796-28S1, R21 AG060267. John F. Disterhoft received payment from Brain Research Foundation for grant review service, and received payment from International Bordeaux Neurocampus Aging Meeting (2018). John F. Disterhoft is an unpaid member of Chicago Methodist Senior Services Board. Craig Weiss, Nicola Bertolino, Daniele Procissi, Quinn C. Smith, Kirsten L. Viola, Samuel C. Bartley have no disclosures.

REFERENCES

1. Alzheimer's Association. 2019 Alzheimer's disease facts and figures. *Alzheimers Dement*. 2019;15(3):321-87. https://doi.org/10.1016/j.jalz.2019.01.010
2. Jack CR Jr, Bennett DA, Blennow K, et al. Contributors. NIA-AA research framework: toward a biological definition of Alzheimer's disease. *Alzheimers Dement*. 2018;14(4):535-562.
3. Mullard A. FDA approval for Biogen's aducanumab sparks Alzheimer disease firestorm. *Nat Rev Drug Discov*. 2021;20(7):496.
4. Salloway S, Farlow M, McDade E, et al. Dominantly Inherited Alzheimer Network–Trials Unit. A trial of gantenerumab or solanezumab in dominantly inherited Alzheimer's disease. *Nat Med*. 2021;27(7):1187-1196.
5. Jacobsen H, Ozmen L, Caruso A, et al. Combined treatment with a BACE inhibitor and anti-Aβ antibody gantenerumab enhances amyloid reduction in APPLondon mice. *J Neurosci*. 2014;34(35):11621-11630.
6. Cummings JL, Morstorf T, Zhong K. Alzheimer's disease drug-development pipeline: few candidates, frequent failures. *Alzheimers Res Ther*. 2014;6(4):37.
7. Cummings J, Lee G, Ritter A, Sabbagh M, Zhong K. Alzheimer's disease drug development pipeline: 2019. *Alzheimers Dement (N Y)*. 2019;5:272-293.
8. Davidson JS, West RL, Kotikalapudi P, Maroun LE. Sequence and methylation in the beta/A4 region of the rabbit amyloid precursor protein gene. *Biochem Biophys Res Commun*. 1992;188(2):905-911.
9. Fan J, Kitajima S, Watanabe T, et al. Rabbit models for the study of human atherosclerosis: from pathophysiological mechanisms to translational medicine. *Pharmacol Ther*. 2015;146:104-119.
10. Vasileva A, Jessberger R. Precise hit: adeno-associated virus in gene targeting. *Nat Rev Microbiol*. 2005;3(11):837-847. Review.
11. Tracy JA, Thompson JK, Krupa DJ, Thompson RF. Evidence of plasticity in the pontocerebellar conditioned stimulus pathway during classical conditioning of the eyeblink response in the rabbit. *Behav Neurosci*. 2013;127(5):676-689.
12. Suter EE, Weiss C, Disterhoft JF. Differential responsivity of neurons in perirhinal cortex, lateral entorhinal cortex, and dentate gyrus during time-bridging learning. *Hippocampus*. 2019;29(6):511-526.
13. Reus-García MM, Sánchez-Campusano R, Ledderose J, et al. The claustrum is involved in cognitive processes related to the classical conditioning of eyelid responses in behaving rabbits. *Cereb Cortex*. 2021;31(1):281-300.
14. Oswald BB, Maddox SA, Tisdale N, Powell DA. Encoding and retrieval are differentially processed by the anterior cingulate and prelimbic cortices: a study based on trace eyeblink conditioning in the rabbit. *Neurobiol Learn Mem*. 2010;93(1):37-45.
15. Woodruff-Pak DS, Finkbiner RG, Sasse DK. Eyeblink conditioning discriminates Alzheimer's patients from non-demented aged. *Neuroreport*. 1990;1(1):45-48.
16. Sparks DL, Schreurs BG. Trace amounts of copper in water induce beta-amyloid plaques and learning deficits in a rabbit model of Alzheimer's disease. *Proc Natl Acad Sci U S A*. 2003;100(19):11065-11069. Epub 2003 Aug 14. Erratum in: Proc Natl Acad Sci U S A. 2003 Sep 30;100(20):11816.
17. Weiss C, Disterhoft JF. Eyeblink conditioning and novel object recognition in the rabbit: behavioral paradigms for assaying psychiatric diseases. *Front Psychiatry*. 2015;6:142.
18. Bertolino N, Procissi D, Disterhoft JF, Weiss C. Detection of memory- and learning-related brain connectivity changes following trace eyeblink-conditioning using resting-state functional magnetic resonance imaging in the awake rabbit. *J Comp Neurol*. 2021;529(7):1597-1606.
19. Ghadery C, Pirpamer L, Hofer E, et al. R2* mapping for brain iron: associations with cognition in normal aging. *Neurobiol Aging*. 2015;36(2):925-932.
20. Ronald JA, Chen Y, Bernas L, et al. Clinical field-strength MRI of amyloid plaques induced by low-level cholesterol feeding in rabbits. *Brain*. 2009;132(Pt 5):1346-1354.
21. Woodruff-Pak DS, Lavond DG, Logan CG, Thompson RF. Classical conditioning in 3-, 30-, and 45-month-old rabbits: behavioral learning and hippocampal unit activity. *Neurobiol Aging*. 1987;8(2):101-108.
22. Thompson LT, Moyer JR Jr, Disterhoft JF. Trace eyeblink conditioning in rabbits demonstrates heterogeneity of learning ability both between and within age groups. *Neurobiol Aging*. 1996;17(4):619-629.
23. Moyer JR, Deyo RA, Disterhoft JF. Hippocampectomy disrupts trace eye-blink conditioning in rabbits. *Behav Neurosci*. 1990;104(2):243-252.
24. Weiss C, Procissi D, Power JM, Disterhoft JF. The rabbit as a behavioral model system for magnetic resonance imaging. *J Neurosci Methods*. 2018;300:196-205.
25. Lambert MP, Velasco PT, Chang L, et al. Monoclonal antibodies that target pathological assemblies of abeta. *J Neurochem*. 2007;100(1):23-35.
26. Nägga K, Gustavsson AM, Stomrud E, et al. Increased midlife triglycerides predict brain β-amyloid and tau pathology 20 years later. *Neurology*. 2018;90(1):e73-e81.
27. Barker GR, Warburton EC. When is the hippocampus involved in recognition memory? *J Neurosci*. 2011;31(29):10721-10731.
28. Norman G, Eacott MJ. Impaired object recognition with increasing levels of feature ambiguity in rats with perirhinal cortex lesions. *Behav Brain Res*. 2004;148(1-2):79-91.
29. Bussey TJ, Muir JL, Aggleton JP. Functionally dissociating aspects of event memory: the effects of combined perirhinal and postrhinal cortex lesions on object and place memory in the rat. *J Neurosci*. 1999;19(1):495-502.
30. Warburton EC, Brown MW. Neural circuitry for rat recognition memory. *Behav Brain Res*. 2015;285:131-139.
31. McCormick DA, Thompson RF. Cerebellum: essential involvement in the classically conditioned eyelid response. *Science*. 1984;223:296-299.
32. Yeo CH, Hardiman HJ, Glickstein M. Classical conditioning of the nictitating membrane response of the rabbit I. Lesions of the cerebellar nuclei. *Exp Brain Res*. 1985;60:87-98.
33. Solomon PR, Vander Schaaf ER, Thompson RF, Weisz DJ. Hippocampus and trace conditioning of the rabbit's classically conditioned nictitating membrane response. *Behav Neurosci*. 1986;100:729-744.
34. Moyer JR, Deyo RA, Disterhoft JF. Hippocampal lesions impair trace eye-blink conditioning in rabbits. *Behav Neurosci*. 1990;104:243-252.
35. Kim JJ, Clark RE, Thompson RF. Hippocampectomy impairs the memory of recently, but not remotely, acquired trace eyeblink conditioned responses. *Behav Neurosci*. 1995;109:195-203.
36. Woodruff-Pak DS, Logan CG, Thompson RF. Neurobiological substrates of classical conditioning across the life span. *Ann N Y Acad Sci*. 1990;608:150-173.
37. Knuttinen MG, Power JM, Preston AR, Disterhoft JF. Awareness in classical differential eyeblink conditioning in young and aging humans. *Behav Neurosci*. 2001;115(4):747-757.
38. Schroeder MP, Weiss C, Procissi D, Disterhoft JF, Wang L. Intrinsic connectivity of neural networks in the awake rabbit. *Neuroimage*. 2016;129:260-267.
39. Lin L, Fu Z, Jin C, Tian M, Wu S. Small-world indices via network efficiency for brain networks from diffusion MRI. *Exp Brain Res*. 2018;236(10):2677-2689.
40. Lee BR, Miller JM, Yang CY, et al. Amino acid sequence of rabbit apolipoprotein E. *J Lipid Res*. 1991;32(1):165-171.
41. Conaway HH, Brown CJ, Sanders LL, Cernosek SF, Farris HE, Roth SI. Spontaneous diabetes mellitus in the New Zealand white rabbit: history, classification, and genetic analysis. *J Hered*. 1980;71(3):179-186.

42. Ning B, Wang X, Yu Y, et al. High-fructose and high-fat diet-induced insulin resistance enhances atherosclerosis in Watanabe heritable hyperlipidemic rabbits. *Nutr Metab (Lond)*. 2015;12:30.
43. Yamamoto T, Bishop RW, Brown MS, Goldstein JL, Russell DW. Deletion in cysteine-rich region of LDL receptor impedes transport to cell surface in WHHL rabbit. *Science*. 1986;232(4755):1230-1237.
44. Shiomi M, Koike T, Ito T. Contribution of the WHHL rabbit, an animal model of familial hypercholesterolemia, to elucidation of the anti-atherosclerotic effects of statins. *Atherosclerosis*. 2013;231(1):39-47.
45. Chen Y, Lim P, Rogers KA, Rutt BK, Ronald JA. In vivo MRI of amyloid plaques in a cholesterol-fed rabbit model of Alzheimer's disease. *J Alzheimers Dis*. 2018;64(3):911-923.
46. Underwood EL, Thompson LT. A high-fat diet causes impairment in hippocampal memory and sex-dependent alterations in peripheral metabolism. *Neural Plast*. 2016;2016:7385314.
47. Underwood EL, Thompson LT. High-fat diet impairs spatial memory and hippocampal intrinsic excitability and sex-dependently alters circulating insulin and hippocampal insulin sensitivity. *Biol Sex Differ*. 2016;7:9.
48. Marwarha G, Dasari B, Prasanthi JR, Schommer J, Ghribi O. Leptin reduces the accumulation of abeta and phosphorylated tau induced by 27-hydroxycholesterol in rabbit organotypic slices. *J Alzheimers Dis*. 2010;19(3):1007-1019.
49. Luchsinger JA, Zetterberg H. Tracking the potential involvement of metabolic disease in Alzheimer's disease-biomarkers and beyond. *Int Rev Neurobiol*. 2020;154:51-77.
50. Rozema NB, Procissi D, Bertolino N, et al. Aβ oligomer induced cognitive impairment and evaluation of ACU193-MNS-based MRI in rabbit. *Alzheimers Dement (N Y)*. 2020;6(1):e12087.

How to cite this article: Weiss C, Bertolino N, Procissi D, et al. Diet-induced Alzheimer's-like syndrome in the rabbit. *Alzheimer's Dement*. 2022;8:e12241. https://doi.org/10.1002/trc2.12241